

## Studies on SST pointing models

M. Y. Kagohara<sup>1</sup> & C. G. G. Castro<sup>1</sup>

<sup>1</sup> CRAAM, Escola de Engenharia, Universidade Presbiteriana Mackenzie, São Paulo, Brasil  
e-mail: myrnayk@protonmail.com, guigue@craam.mackenzie.br

**Abstract.** Solar Submillimeter Telescope is a radio telescope installed at Casleo (*Complejo Astronomico El Leoncito*) for observing solar flares, fitted with four channels operating at 212 GHz and two at 405 GHz. This article describes the assessment of SST pointing precision using Tpoint, a commercial software package, based on 20 years of observational data, from 1999 to 2019. After an initial analysis based on the geometric features of SST, there were additional studies with terms related to physical effects, then adding empirical corrections to the model with best results. Also, the pointing analysis was made separately for AM and PM data, resulting in somewhat different pointing models for each period. Recommendations for SST improvement are given based on the results of this work.

**Resumo.** O SST (Telescópio solar para ondas submilimétricas) é um radio-telescópio instalado no Casleo (*Complejo Astronomico El Leoncito*) para observação de explosões solares, provido de quatro canais que operam a 212 GHz e dois a 405 GHz. Este artigo descreve a avaliação da precisão de apontamento do SST usando Tpoint, um software comercial, com base em 20 anos de dados observacionais. Depois de uma análise inicial baseada nas características geométricas do SST, houve estudos adicionais com termos relacionados aos efeitos físicos, e então com a adição de correções empíricas ao modelo que apresentou os melhores resultados. Além disso, foi feita uma análise de apontamento para dados AM e PM separadamente, resultando em modelos de apontamento significativamente diferentes para cada período. São feitas recomendações de melhoria do SST com base nos resultados deste trabalho.

**Keywords.** Telescope – Sun: flares – Submillimeter: general

### 1. Introduction

The observation of the Sun in the centimetric, millimetric and sub-millimetric wavelengths allows a detailed study of solar flares. With this purpose, the SST (Solar Submillimeter Telescope) (Kaufmann 2008) is installed at Casleo (*Complejo Astronomico El Leoncito*) and operates at 212 and 405 GHz radio frequencies (Castro 2018).

The SST's multibeam focal arrangement is fitted with four channels operating at 212 GHz, and two channels operating at 405 GHz. Channels 2 to 4 partially overlap at 3 dB, making possible the comparison of antenna temperatures during solar eruptive events and the determination of the centroid of flare radiation emission. All the detectors of these channels are installed under the backplane of the primary reflector. The telescope mount is of altazimuth type (precision of 1.8 arcsec). A typical SST work scan is given in Figure 1. Besides solar ob-

servations, temperature calibration and studies on atmospheric transparency (Espinoza 2017) are also done using SST.

Because it operates at such high operation frequencies, the size of its beam is relatively small. Additionally, due to the process of radio imaging (which is based on scanning the solar disc and surrounding area with the beam), and because solar flares occur in a relatively short time scale, the SST must be moved at high speeds. These operational features impose stringent pointing precision requirements.

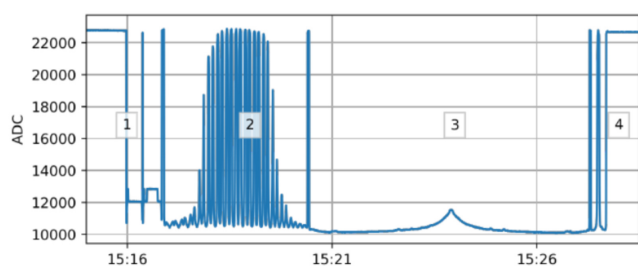
This work aims to analyze the SST accuracy using pointing models on Tpoint software suite (Tpoint 2006), based on the observational data already available.

### 2. Development and Methodology

Meeks (1968) and Mangum (2006) describe calibration and pointing methods for radio telescopes. The former was applied to SST in its first version. In November, 2006, SST was overhauled (Kaufmann 2008) for improvements on the main reflector and the pointing accuracy; at that time, Tpoint (2006) has been deployed on the telescope control system, and the pointing calibration method became similar to the latter.

Menezes (2017, 2021), in his research, collected and analyzed SST data from its first light to 2019. He obtained solar maps by analysing part 2 of the SST scan (see Figure 1), then could get information on the offset of the solar disc center from the pointing target of the telescope. Based on these reduced data, the authors of this work perform the SST pointing analysis for each season of every year, calculating a pointing model and residual pointing errors for the related time slots. Time references from NASA Goddard (n.d.) are used in the SST operation. Equinox and solstice dates from this same source are used for limiting the ranges for each observational analysis.

Since the 405 GHz instrumentation has reached the end of its work life, this work focused on analyzing the solar maps made at



1. Temperature calibration  
2. Solar map scan  
3. Atmospheric opacity ( $\tau$ ) scan  
4. Scan of the Sun map center, followed by a scan on a special region of interest (usually an active region on the Sun).

FIGURE 1. SST operation scan. Source: Menezes (2017)

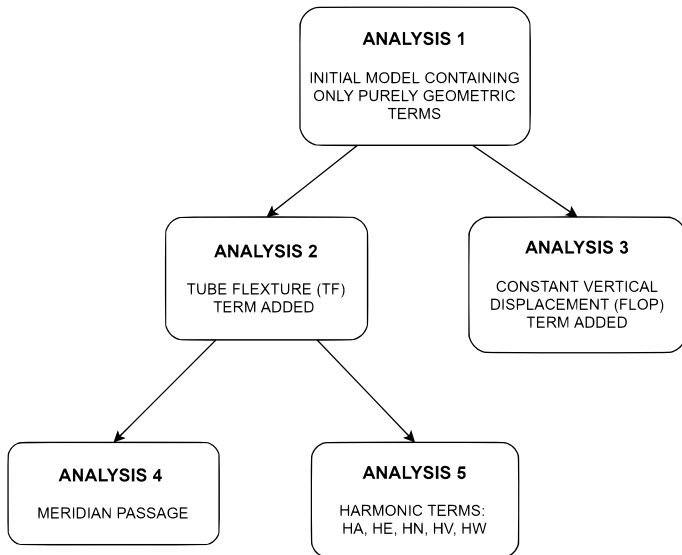


**FIGURE 2.** Analysis of the SST pointing models and their effects on SST accuracy

**TABLE 1.** Terms of the initial SST pointing model.

Term	Effect	Applies to
IA	Azimuth zero-point error	SST
IE	Elevation zero-point error	Each channel
NPAE	Non-perpendicularity between azimuth and elevation axes	SST
CA	Left-right collimation error	Each channel
AN	Azimuth axis misalignment in the N-S direction	SST
AW	Azimuth axis misalignment in the E-W direction	SST

212 GHz. We use Tpoint commercial software to analyze solar maps obtained from SST observational data, aiming to reduce pointing error by using different sets of pointing model parameters.

For each season, in each analysis, a pointing model was determined for the selected terms. A total of 780 pointing models was calculated, and a sample of these models can be seen on Table 3. Tpoint also provided, for each model, sets of RMS values for N-S, E-W, left-right, up-down directions, and for the whole sky. The pointing performance is based on the analysis of such RMS values.

This work was based initially on the data available for SST’s first light (1999) to the Spring of 2019. Figure 3 shows a chart of residual pointing deviations after applying the initial model, and highlights the range of interest adopted for further analysis. Blanks in the graph refer to unavailable data. On the graph, blue bars represent the pointing deviation RMS in E-W direction; orange bars: for N-S direction; gray bars, for left-right direction; yellow bars: for up-down direction. Finally, the blue line represents the pointing deviation RMS for the whole sky.

The lower limit of the range of interest was defined as the point at which the SST operation became steady. From the first light (1999) to 2005, SST’s pointing system was based on the methodology described by (Meeks 1968). On November, 2006, the telescope was repaired and upgraded, and Tpoint (Tpoint 2006) was deployed for pointing calibration and, from that occasion, the graph shows remarkable improvements in pointing ac-

**TABLE 2.** Tpoint terms selected for detailed analysis.

Term	Effect
TF	Flexure of the telescope tube, supposing that its behavior can be modeled using the Hooke’s law.
FLOP	Constant vertical displacement.
HA	Group of harmonic terms for empirical correction in azimuth, that are proportional to sine/cosine of elevation/azimuth.
HE	Group of harmonic terms for empirical correction in elevation, that are proportional to sine/cosine of elevation/azimuth.
HN	Group of harmonic terms for empirical correction that tilts the azimuth axis in the N-S direction, that are proportional to sine/cosine of elevation/azimuth.
HV	Group of harmonic terms for empirical correction that changes the perpendicularity error between elevation and azimuth axis, that are proportional to sine/cosine of elevation/azimuth.
HW	Group of harmonic terms for empirical correction that tilts the azimuth axis in the E-W direction, that are proportional to sine/cosine of elevation/azimuth.

curacy and repeatability. So, for further analysis, data acquired before the summer solstice of 2006 were not used.

The upper limit was chosen as the point at which software precision constraints arose due to the end of the applicability limit of IERS data tables provided by (NASA Goddard n.d.), which were used for calculations of date and time in the SST control system, based on astropy library. While running the analysis code, a warning was issued to inform about the possibility of positional errors with a magnitude of arcsecs.

The analysis process is shown on Figure 2. ANALYSIS 1 applies the initial SST pointing model to a seasonal accuracy analysis from the first light (1999) to the 2019 summer solstice, with the results shown on Figure 3. Tpoint terms selected for use are shown on Table 1.<sup>1</sup> CA and IE terms are applicable to each of the 212 GHz channels, and IA, NPAE, AN, and AW are applicable to the telescope mount, i. e., to the SST as a whole.

Then, ANALYSIS 2 to ANALYSIS 5 were based on observational data in the range of interest shown on Figure 3. Initially, separate studies on the impact of TF (tube flexure) and FLOP (constant vertical displacement) terms were done in ANALYSIS 2 and ANALYSIS 3, respectively. Given the better performance of the former, in-depth studies on the model with TF were made: ANALYSIS 4 dealt with separate studies for AM and PM data with no other terms added to the pointing model; and ANALYSIS 5 investigated the possibility of further improvements in pointing accuracy using empirical corrections, in the form of harmonic terms. A description of each term used in these further analyses can be seen on Table 2. Figure 4 shows how each seasonal analysis, for each pointing model, is done with the aid of Tpoint.

### 3. Results

Figure 3 shows the results of the preliminary analysis, already discussed in Section 2, which provided the foundation for the in-depth analysis of the SST pointing performance.

Figure 5 shows the results of ANALYSIS 2, 3, and 5. Adding FLOP to the pointing model did not result in significant im-

<sup>1</sup> Complete information on how each pointing term unfolds into azimuth and elevation corrections can be seen on Tpoint (2006).

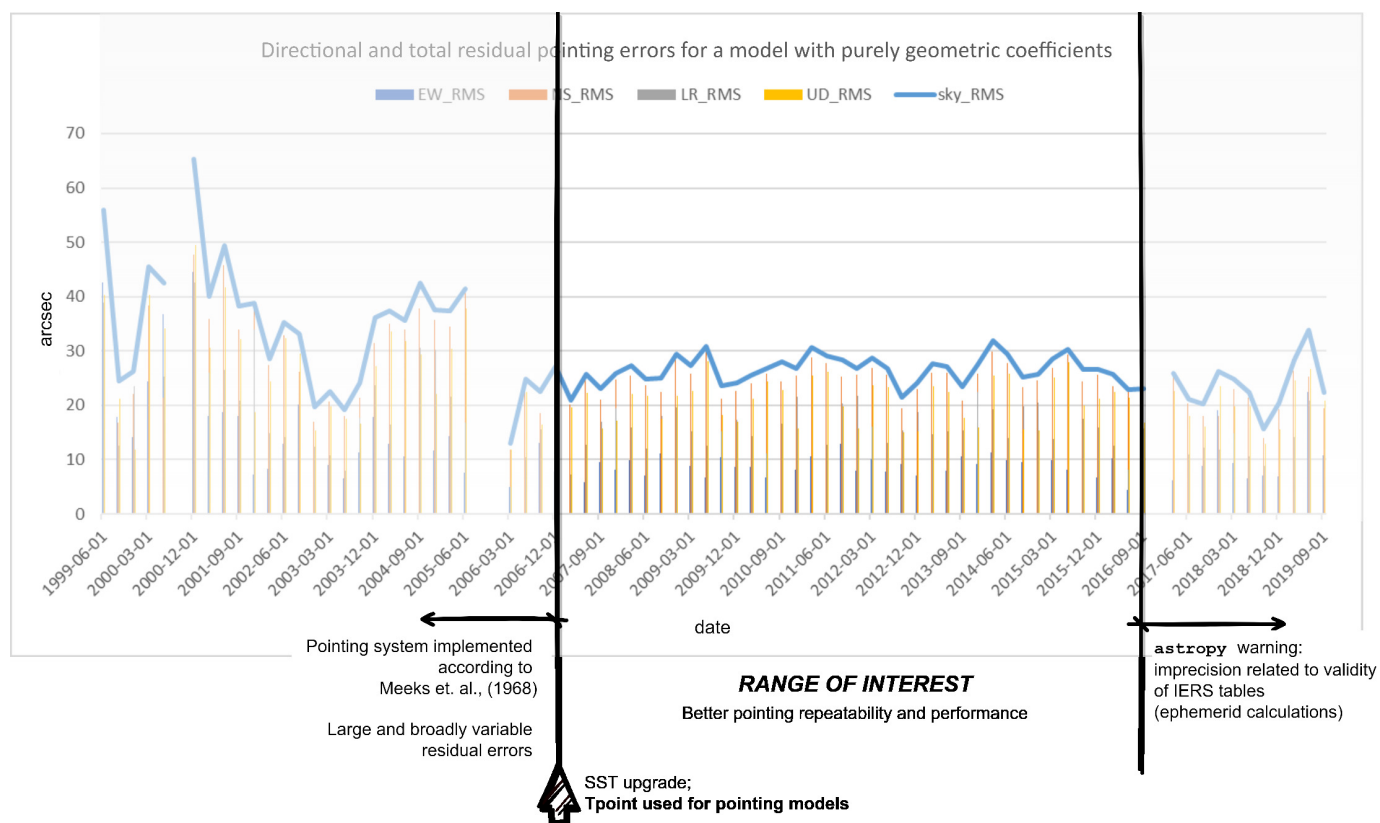


FIGURE 3. RMS for the whole sky and for each direction for the initial pointing model (purely geometrical terms) applied to the solar maps from 1999 to the summer solstice of 2019; with the chosen range of interest for further study.

TABLE 3. Statistical parameters of RMS values (in arcsec) for each pointing model.

Param.	RMS Basic model	RMS w/FLOP	RMS w/TF	RMS w/TF+HA	RMS w/TF+HE	RMS w/TF+HN	RMS w/TF+HV	RMS w/TF+HW	RMS AM	RMS PM
MEAN	26.49	26.49	26.40	26.29	26.33	26.27	26.33	26.29	25.52	25.94
MIN	20.94	20.94	20.94	20.91	20.93	20.85	20.91	20.80	12.07	17.20
MAX	31.87	31.87	31.81	31.75	31.79	31.76	31.77	31.79	33.97	32.40
STD DEV	2.58	2.58	2.63	2.66	2.64	2.67	2.65	2.67	4.45	3.52

Note: The last two columns refer to pointing models applied separately for observational data collected before the meridian passage (AM model) and after the meridian passage (PM model) at the Casleo site, which is approximately 15UTC.

TABLE 4. Percent values and statistic parameters for the differences between the RMS values for each pointing model and the RMS for the basic model.

Param.	RMS w/FLOP - Basic	RMS w/TF - Basic	RMS w/TF+HA- Basic	RMS w/TF+HE- Basic	RMS w/TF+HN- Basic	RMS w/TF+HV- Basic	RMS w/TF+HW- Basic	RMS AM - Basic	RMS PM - Basic
MEAN	0.00	-0.09	-0.20	-0.16	<b>-0.22</b>	-0.16	-0.20	-0.97	-0.55
% variation	0.00	0.00	-0.01	-0.01	<b>-0.01</b>	-0.01	-0.01	-0.04	-0.02
MIN	0.00	-1.11	-1.15	-1.18	-1.40	-1.29	-1.40	-9.85	-5.71
MAX	0.02	0.00	-0.01	-0.01	-0.01	0.00	0.00	6.66	3.05
STD DEV	0.00	0.21	0.25	0.22	0.27	0.23	0.25	3.75	1.98

Notes:

1. The last two columns refer to pointing models applied separately for observational data collected before the meridian passage (AM model) and after the meridian passage (PM model) at the Casleo site, which is approximately 15UTC.
2. Negative values show that the model specified at the table header has a lower RMS value than the basic model of this analysis.

provements. With the addition of TF, no significant improvement could be seen before the summer solstice of 2015. After this date, however, TF usage improves the pointing performance of SST. Possibly, the compensation of flexure of the telescope became necessary only after wear of the equipment.

The results of ANALYSIS 4 are shown on Figure 6, where it can be seen that the RMS values for AM and PM models for a given set of maps are somewhat different, providing indications that using separate models for AM and PM observations could produce more accurate pointing. It can also be noted that PM values follow the general trends of whole-day models.

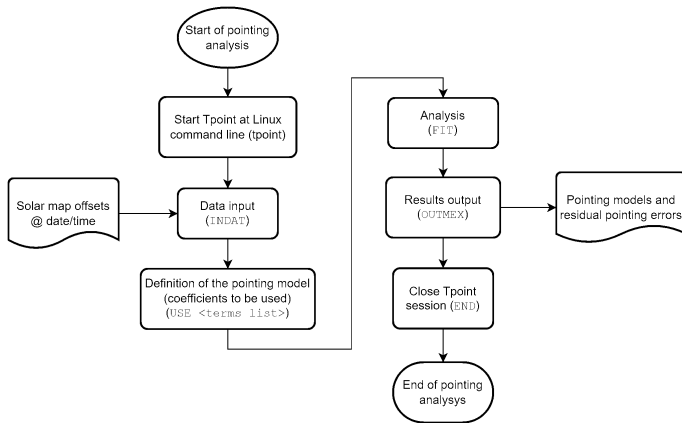


FIGURE 4. Tpoint operation flowchart.

Table 3 shows the values of mean, minimum, and maximum values of the RMS of residual pointing errors obtained after a seasonal analysis, using the correction types linked to some of the Tpoint terms. It can be seen that the RMS values for the whole sky varies from 20.8 to 31.8 for whole-day pointing models, with standard deviation values ranging from 2.58 to 2.67 arcsec. For models that were calculated separately for AM and PM solar maps (15UTC at Casleo site), the standard deviation values were much higher than those for the whole-day models.

Table 4 shows percentual values and statistical parameters of the variations of RMS values from the basic model. In average, the pointing model used in Analysis 2, that applies a correction related to a flexure modelled according to Hooke's law (parameter TF), with additional correction in the N-S direction (HN-type harmonic parameters), results in the lowest residual pointing errors.

#### 4. Final Remarks

With the results from the analysis of SST pointing models, some possible improvement points could be identified. For example, it was possible to note that the SST was subject to more elastic flexure in the summer of 2015 and the winter of 2016. The model that applies a correction of this effect is able to improve the pointing precision by about 1 arcsec.

The FLOP pointing term for compensating a fixed vertical displacement, which can be related to backlash in the mount parts, showed that such backlash, if existing, do not have an effect on the SST pointing accuracy. First order harmonic terms were useful for reducing the residual pointing deviations for all cases. However, they are able to improve pointing accuracy only by less than 1

For further reducing the pointing deviation, future works might focus on:

- Further applying empirical corrections in the N-S directions, using higher order harmonics, or polynomial terms.
- Refurbish the mechanical structure of the SST mount, with a higher priority for subsystems and parts related to N-S and up-down directions.

Separate analysis for AM and PM solar maps suggests that the use of different calibrations for each half of the day might be valid for increased pointing accuracy. Also, the accuracy of the time references used for calculations is also a point to be further investigated.

*Acknowledgements.* The authors want to express their gratitude to *Instituto Presbiteriano Mackenzie*, *Mackpesquisa* Fund, CAPES, Fapesp, and CNPq,

for the generous financial support; and also to the operations on *Complejo Astronomico El Leoncito*, realized under agreement between *Consejo Nacional de Investigaciones Científicas y Técnicas de la República Argentina* and La Plata, Córdoba, and San Juan Universities, for the wealth of observational data provided for this work.

#### References

- Castro, C.G.G. et.al, The September 6, 2017 X9 super flare observed from submillimeter to Mid-IR, Edited by American Geophysical Union. Space Weather.
- Espinoza, D.V.C., "Determinação da opacidade atmosférica em comprimentos de ondas submilimétricas", Dissertation (Geospatial Sciences and Applications). São Paulo, São Paulo: Universidade Presbiteriana Mackenzie.
- Kaufmann, Pierre, et al., "New telescopes for ground-based solar observations at submillimeter and mid-infrared", Proceedings SPIE 7012, Ground-based and Airborne Telescopes II, 70120L.
- Mangum, J. G., et. al., "Evaluation of the ALMA Prototype Antennas", Publications of the Astronomical Society of the Pacific 118, no. 847.
- Meeks, M. L., Ball, J.A. & Hull, A.B. "The Pointing Calibration of the Haystack Antenna", IEEE Transactions on Antennas and Propagation, 1968, 746.
- Menezes, F.M., "Influência da atividade magnética na atmosfera solar e na propagação de ejeções de massa coronal de estrelas do tipo-solar", thesis (Ciências e Aplicações Geoespaciais), São Paulo, SP: Universidade Presbiteriana Mackenzie, October 4, 2021.
- Menezes, F.M., "Raio solar em frequências subterahertz e sua relação com a atividade solar", dissertation (Geospatial Sciences and Applications), São Paulo, São Paulo: Universidade Presbiteriana Mackenzie.
- NASA Goddard, Time and Date of Vernal Equinox, <https://data.giss.nasa.gov/modelE/ar5plots/srvernal.html>.
- Tpoint Software, TPOINT - A Telescope Pointing Analysis System, product manual.

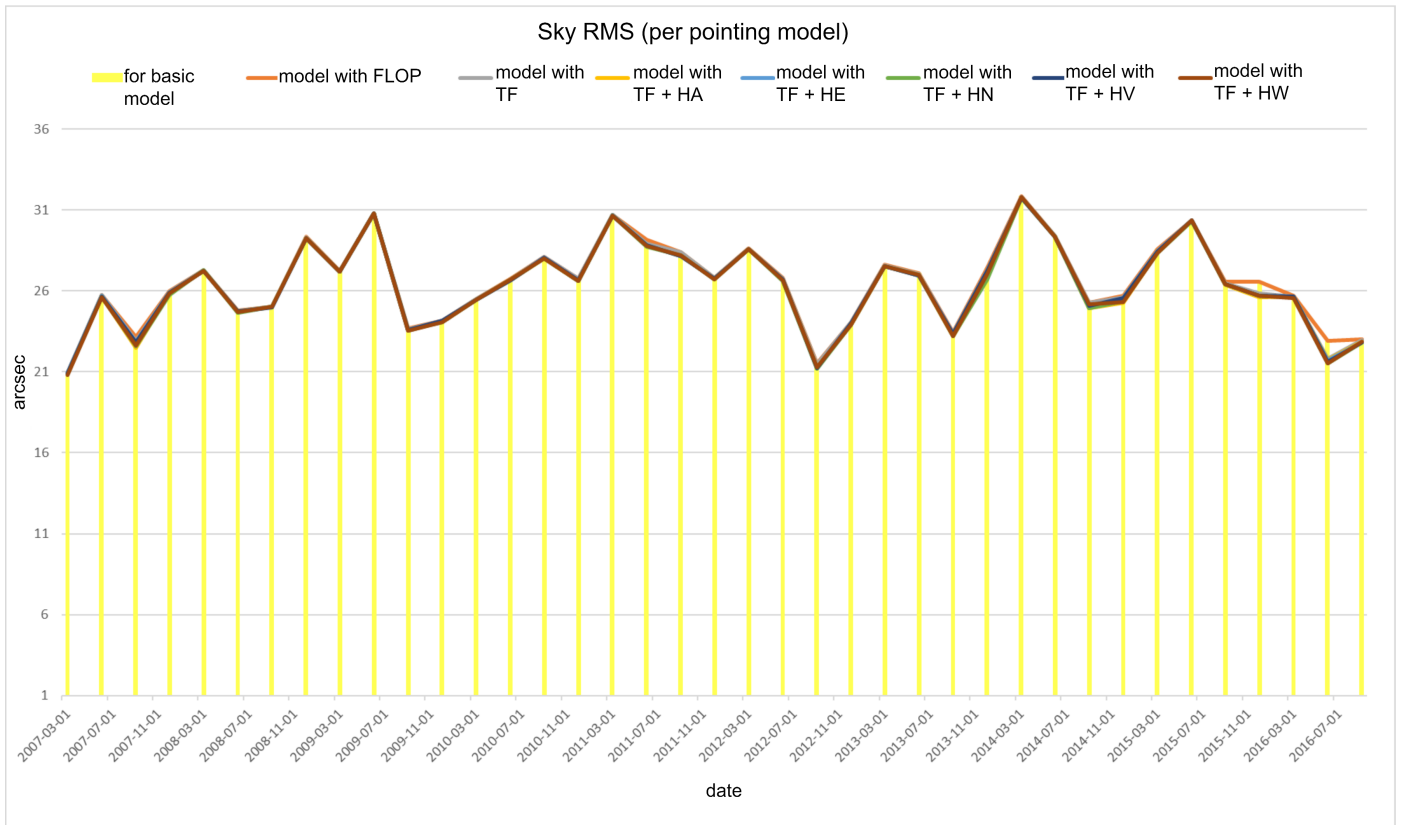


FIGURE 5. Consolidated Graph – RMS when all-day observations taken into account for pointing model calculations.

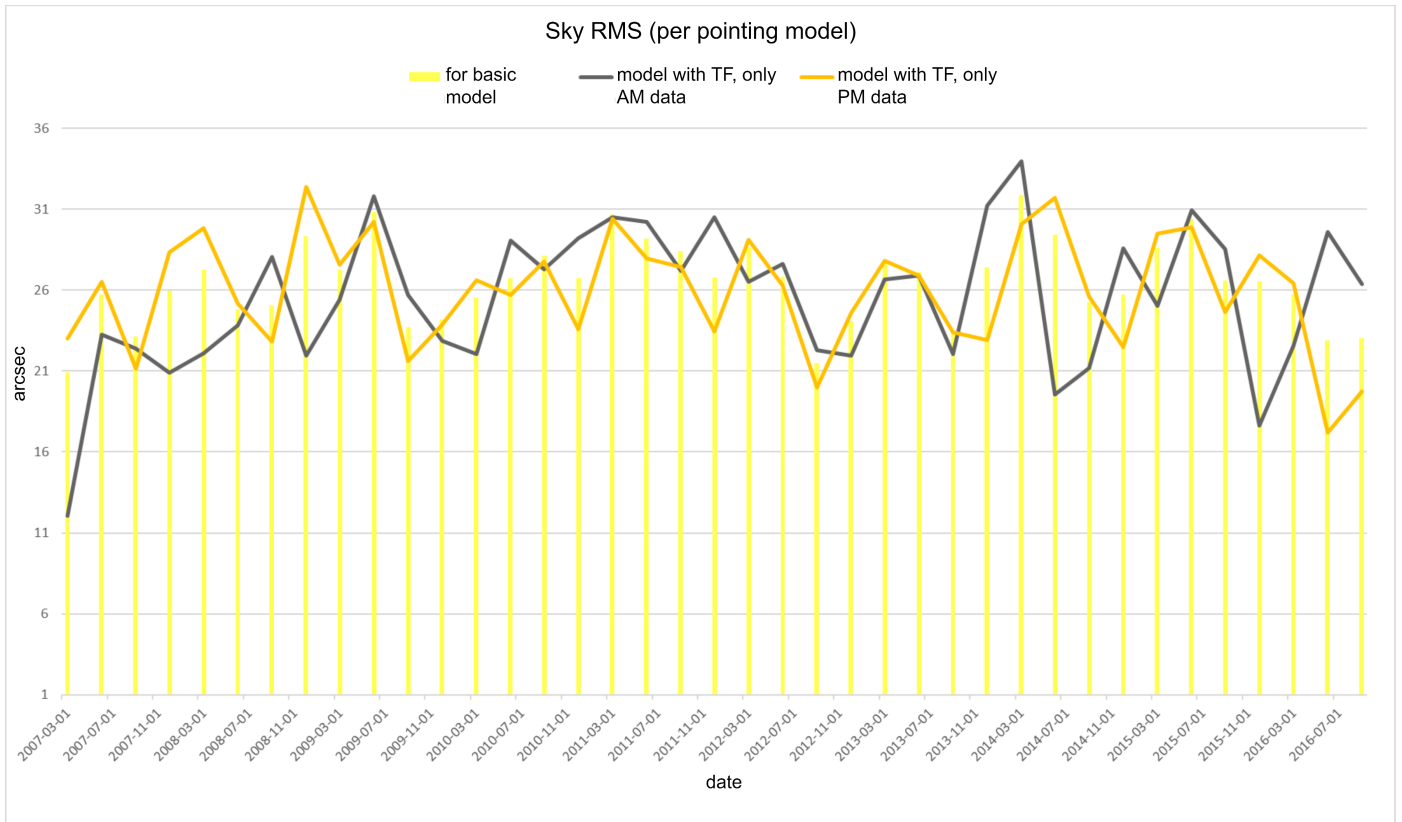


FIGURE 6. Consolidated Graph – RMS for models with TF, for AM and PM observational data.